A Study on Pin-wise Burnup Estimation with Embedded Pin Power Reconstruction

Yunseok Jeong [a], Taesuk Oh [a], Yonghee Kim [a*]
[a]*Nuclear and Quantum Engineering, KAIST*
[*]*Corresponding author: yongheekim@kaist.ac.kr*

Keywords : Pin power reconstruction, embedded calculation, nodal method, depletion

1. Introduction

In modern light water reactor analysis, the two-step method based on simplified equivalence theory is commonly used [1]. For reconstructing the pin-wise power distribution which is lost during homogenization, the form function-based pin power reconstruction (FF-PPR) method has been widely used [2]. This approach is straightforward to implement and does not require noticeable computing burden once the form functions are generated. However, FF-PPR does not account for neighboring assembly effects and burnup gradient within fuel assemblies as it relies on a single lattice calculation under reflective boundary condition.

To address these limitations, an embedded calculation for PPR (EPPR) has recently been introduced [3]. It directly solves a fixed-source problem for extended 2-D color-set geometry using nodal result, pin-wise group constants, and discontinuity factors (DFs). Studies have demonstrated that EPPR is more accurate than FF-PPR, requiring only a marginal increase in computing time in small 2-D benchmark problems. Additionally, it has been shown that EPPR method produces smaller pin-wise power errors than FF-PPR in the depleted core [4]. However, results indicate that the root mean square (RMS) error of pin power increases with core burnup, particularly near reflector regions where steep burnup gradients exist within fuel nodes.

The main objective of this study is to enhance and validate the performance of EPPR in a highly-depleted 2-D benchmark problem by estimating pin-wise burnup values. The reference solutions and group constants are generated using the method of characteristics (MOC) transport code, DeCART2D [5]. The nodal code KANT, developed at KAIST, was employed to generate nodal results and the corresponding reconstructed pin-wise power distributions [6].

2. Methods

2.1 Embedded Pin Power Reconstruction

In EPPR method, the pin-wise power distribution is directly determined by solving heterogeneous diffusion equations within a pin-level domain, which consists of a target fuel node and the surrounding radial buffer zone. The pin power distribution of centered fuel assembly (FA) is obtained using an extended color-set problem. The buffer zone width can be either the full width (EPPR-Full) of the assembly or half of it (EPPR-Half). In this study, a half-width buffer zone is adopted for EPPR scheme to reduce the size of EPPR system matrix, given that the system matrix is typically ill-conditioned. The domain scheme for the EPPR is illustrated in Figure 1. Pin-wise homogenized group constants (HGCs) and DFs are obtained from the reference heterogeneous net current and surface flux obtained through lattice calculations using DeCART2D transport code. For the baffle-reflector regions, pin-wise HGCs and DFs are generated by performing a whole-core pin-wise calculation at zero burnup. In this study, nodal expansion method (NEM) is used to generated pin-wise DFs.

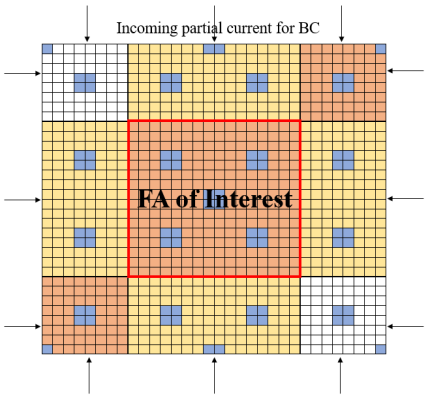

Figure 1. General domain scheme of EPPR-Half

EPPR directly solves two-group diffusion equation in Eq. (1) for the extended color-set problem.

$$\nabla \cdot \vec{J}_g(r) + \Sigma_{r,g}(r)\phi_g(r) = \frac{\chi_g}{k_{eff}} \sum_{g=1}^{2} \nu\Sigma_{f,g}(r)\phi_g(r) - \sum_{g' \neq g}^{2} \Sigma_{s,g' \to g}(r)\phi_{g'}(r), \quad (1)$$

where k_{eff} is the reactor eigenvalue obtained from nodal analysis, and other notations follow standard conventions. The incoming partial currents are used as boundary conditions for numerical stability, where NEM kernel is solved and accelerated by the CMFD method [7]. Then, the CMFD equation for Eq. (1) can be expressed as:

$$\left(A - \frac{1}{k_{eff}} F \right) \Phi = S_{BC} \quad (2)$$

where A is CMFD matrix, Φ is pin-wise flux vector, F is fission matrix, and S_{BC} is boundary source vector.

2.2 Pin-wise Burnup Estimation in EPPR

In burnup calculations, pin-wise burnup values are updated at each burnup step using nodal results and reconstructed pin-wise power. The pin-wise burnup increment is estimated by conventional predictor-corrector method, the detailed procedure is described in Figure 2.

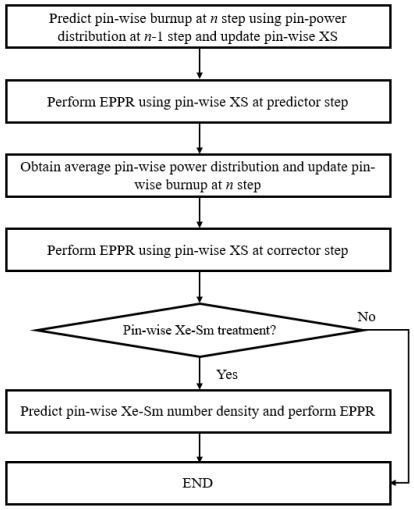

Figure 2. Predictor-corrector scheme for pin-wise burnup estimation

Pin-wise HGCs and DFs for each pin at a certain burnup stage are obtained from the linear interpolation of pin-wise cross section library. This procedure is applied for all types of cross sections except for the absorption cross section, which requires further treatment.

2.3 Absorption Cross Section Estimation in EPPR

As Xe-135 and Sm-149 are accumulated during depletion, the pin-wise absorption cross sections must be adjusted to account for changes in the number densities of these isotopes. The precise number densities are not available without solving pin-wise Xe-135 and Sm-149 number density differential equations. Therefore, this study proposes and compares two methods.

The first method involves using nodal values for pin-wise number densities. However, since the nodal values include the volume of region where no fuel exists, total volume-to-fuel volume ratio must be considered. The relevant equation is presented in Eq. (3). While this is the simplest approach and ensures the conservation of nodal number densities, it does not account for the fact that power varies between individual fuel rods, leading to different number densities of Xe-135 and Sm-149 in each fuel rod.

$$\begin{aligned}\Sigma_{ab,g,x,y,z,i,j} &= \Sigma^{0}_{ab,g,x,y,z,i,j} \\ &+(N_{Xe,x,y,z}\sigma_{Xe,g,x,y,z,i,j} + N_{Sm,x,y,z}\sigma_{Sm,g,x,y,z,i,j}) \\ &\times \frac{V_{total}}{V_{total}-V_{guide}}\end{aligned} \tag{3}$$

where g is the energy group, $\Sigma^{0}_{ab,g,x,y,z,i,j}$ is the pin-wise absorption cross section without Xe-135 and Sm-149, $N_{Xe,x,y,z}$ is the node-averaged number density of Xe-135, $N_{Sm,x,y,z}$ is the node-averaged number density of Sm-149, $\sigma_{Xe,g,x,y,z,i,j}$ and $\sigma_{Sm,g,x,y,z,i,j}$ are pin-wise homogenized microscopic absorption cross section of Xe-135 and Sm-149, V_{total} is the node volume, and V_{guide} is the total volume of pins which consist of guide tubes.

The second method involves directly calculating the equilibrium number densities using the microscopic cross-section and neutron flux obtained from EPPR. Xe-135 reaches equilibrium in approximately three days, while Sm-149 takes about 21 days. Given that the typical interval between burnup steps in core calculations ranges from several days to over 10 days, it is assumed that the number densities are in equilibrium at each burnup step. However, the average number density of Xe-135 and Sm-149 across individual fuel rods does not guarantee the preservation of the original nodal values. The error can be particularly large in the early stages of burnup. Therefore, the final number densities are adjusted using scaling factor, which is the ratio of two values. In typical two-energy group calculations, the equilibrium number densities can be estimated by using Eq. (4).

$$\begin{aligned}N_{Xe,x,y,z,i,j} &= \frac{(\gamma_I+\gamma_{Xe})(\bar{\Sigma}_{f,1}\phi_F+\bar{\Sigma}_{f,2}\phi_T)}{\lambda_{Xe}+\bar{\sigma}_{a1,Xe}\phi_F+\bar{\sigma}_{a2,Xe}\phi_T} \\ N_{Sm,x,y,z,i,j} &= \frac{(\gamma_{Pm}+\gamma_{Sm})(\bar{\Sigma}_{f,1}\phi_F+\bar{\Sigma}_{f,2}\phi_T)}{(\bar{\sigma}_{a1,Sm}\phi_F+\bar{\sigma}_{a2,Sm}\phi_T)},\end{aligned} \tag{4}$$

where F means fast group, T is thermal group and others are standard. Then, scaling factors are multiplied to corresponding number density to obtain final number densities. Scaling factors can be simply obtained using Eq. (5).

$$f^{Xe}_{x,y,z} = \frac{N_{Xe,x,y,z}}{\sum_{i,j} N_{Xe,x,y,z,i,j}}, f^{Sm}_{x,y,z} = \frac{N_{Sm,x,y,z}}{\sum_{i,j} N_{Sm,x,y,z,i,j}} \tag{5}$$

2.4 Form Function-based PPR

For comparison, FF-PPR is applied in the conventional manner, where the node-wise homogeneous flux distribution is obtained using node surface net currents and corner point fluxes [2]. DeCART2D transport code was employed to generate form functions through lattice calculations. In the depletion analysis, a burnup-dependent form function was applied to each node. After calculating the node-

wise homogeneous flux distribution, the homogeneous power distribution can be obtained with node-wise fission cross section. Then, the predetermined power form function is multiplied to each homogeneous power distribution to reconstruct heterogeneous power distribution, which can be simply expressed in Eq. (6).

$$P_{het}(x,y) = \mathrm{FF}(x,y) \times P_{hom}(x,y) \tag{6}$$

3. Numerical Results

For the numerical benchmark, KAIST-1A 2-D UOX reactor model is tested. The benchmark problem includes three types of 16x16 UOX fuel assemblies, as illustrated in Figure 2. Conventional two-step method was utilized to generate nodal results.

The comparison includes an analysis of nodal accuracy, RMS error in pin power, maximum error in pin power, minimum error in pin power, and relative error in pin burnup. It considers both the EPPR method, with and without Xe-Sm treatment, as well as the FF-PPR method. The relative error in pin burnup is plotted for the fuel assembly with the highest RMS error at each burnup step when EPPR with Xe-Sm treatment is utilized. The pin power reconstruction was conducted at three burnup stages: 0GWD/tU, 15GWD/tU and 30GWD/tU, both of which represent highly depleted subcritical cores. The results are enumerated through subsection 3.1 to 3.3. The burnup step intervals are set as follows:

- 0.10GWD/tU from 0.0GWD/tU to 1.0GWD/tU,
- 0.50GWD/tU from 1.0GWD/tU to 5.0GWD/tU,
- 1.00GWD/tU from 5.0GWD/tU to 30.0GWD/tU.

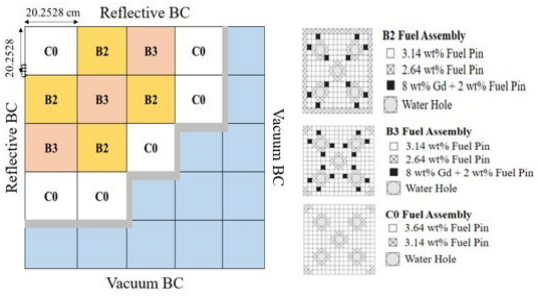

Figure 3. Core Configuration of Benchmark

The analysis at three burnup points indicates that the nodal calculations, crucial for accurate pin power reconstruction, maintain acceptable error margins in both reactivity and assembly power. The EPPR method, in particular, provides more accurate reconstructed pin power, especially in regions near the radial reflector. It not only achieves a lower RMS error but also exhibits smaller errors in both maximum and minimum pin power values.

3.1 0GWD/tU

3.3117	**1.5652**	**0.8138**	**0.6084**
0.637%	-0.141%	-0.946%	0.773%
	1.0353	**0.6605**	**0.4319**
	-1.082%	-0.076%	0.278%
		0.4936	
		-0.182%	

Ref. FA Power
Nodal Error
Reactivity (Error in pcm)
1.074921 (113.9)

Figure 4. Nodal Error at 0GWD/tU

RMS (EPPR)

0.674%	0.290%	0.968%	0.940%
	1.093%	0.221%	0.727%
		0.715%	

Max (EPPR)

-0.092%	0.767%	1.286%	1.074%
	1.372%	0.530%	2.066%
		1.889%	

Min (EPPR)

-0.919%	-0.429%	0.020%	-1.397%
	0.221%	-0.495%	-1.131%
		-0.816%	

Figure 5. Pin Power Error of EPPR at 0GWD/tU

RMS (FF)

1.285%	1.767%	1.676%	1.724%
	1.944%	1.641%	3.070%
		2.977%	

Max (FF)

2.603%	6.903%	6.275%	3.478%
	6.084%	6.633%	21.243%
		17.865%	

Min (FF)

-5.297%	-3.849%	-2.785%	-6.671%
	-1.829%	-4.239%	-8.359%
		-8.171%	

Figure 6. Pin Power Error of FF-PPR at 0GWD/tU

Additionally, when comparing cases with and without Xe-Sm treatment, only marginal change in accuracy was observed. This suggests that even without additional calculation, a simple estimation of Xe-135 and Sm-149 number densities can yield sufficiently accurate pin power results.

3.2 15GWD/tU

1.2408	**1.1999**	**1.1688**	**0.8467**
0.177%	0.017%	0.094%	0.012%
	1.2064	**1.0303**	**0.6562**
	0.149%	-0.039%	-0.183%
		0.749	
		-0.454%	

Ref. FA Power
Nodal Error
Reactivity (Error in pcm)
0.96029 (149)

Figure 7. Nodal Error at 15GWD/tU

RMS (EPPR)

0.535%	0.549%	0.118%	0.824%
	0.165%	0.169%	0.825%
		0.702%	

Max (EPPR)

0.791%	-0.245%	0.354%	1.408%
	0.230%	0.207%	1.262%
		0.874%	

Min (EPPR)

-0.796%	-1.478%	-0.176%	-2.125%
	-0.305%	-1.488%	-1.541%
		-1.905%	

Figure 8. Pin Power Error of EPPR at 15GWD/tU

RMS (EPPR)

0.588%	0.547%	0.183%	0.858%
	0.235%	0.183%	0.870%
		0.739%	

Max (EPPR)

0.913%	-0.163%	0.447%	1.534%
	0.363%	0.319%	1.386%
		0.974%	

Min (EPPR)

-0.956%	-1.404%	-0.302%	-2.275%
	-0.444%	-1.526%	-1.578%
		-1.939%	

Figure 9. Pin Power Error of EPPR w/o treatment at 15GWD/tU

RMS (FF)

1.573%	1.353%	1.564%	3.457%
	1.512%	1.948%	4.329%
		4.369%	

Max (FF)

4.011%	3.904%	4.313%	8.269%
	4.394%	4.718%	15.001%
		11.501%	

Min (FF)

-7.858%	-5.751%	-7.522%	-9.665%
	-7.425%	-7.175%	-10.422%
		-10.720%	

Figure 10. Pin Power Error of FF-PPR at 15GWD/tU

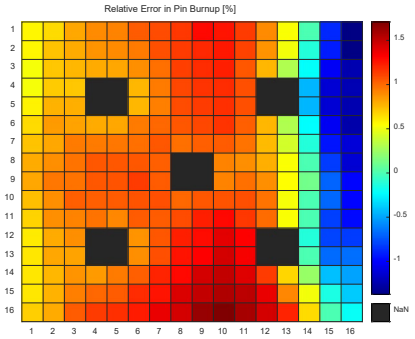

Figure 11. Pin Burnup Error of EPPR at 15GWD/tU

3.3 30GWD/tU

1.1752	**1.1394**	**1.1268**	**0.8975**
0.485%	0.167%	0.160%	-0.056%
	1.1447	**1.0381**	**0.7332**
	0.367%	-0.347%	-0.314%
		0.8101	
		-0.555%	

Ref. FA Power
Nodal Error
Reactivity (Error in pcm)
0.84949 (115.16)

Figure 12. Nodal Error at 30GWD/tU

RMS (EPPR)

0.460%	0.478%	0.260%	1.000%
	0.181%	0.569%	1.063%
		1.107%	

Max (EPPR)

1.637%	-0.098%	0.538%	1.694%
	0.444%	-0.102%	1.770%
		1.934%	

Min (EPPR)

-0.373%	-1.507%	-0.790%	-3.372%
	-0.238%	-3.406%	-3.613%
		-4.155%	

Figure 13. Pin Power Error of EPPR at 30GWD/tU

RMS (EPPR)

0.545%	0.455%	0.304%	1.014%
	0.285%	0.552%	1.072%
		1.102%	

Max (EPPR)

1.802%	-0.004%	0.701%	1.786%
	0.596%	-0.028%	1.891%
		1.987%	

Min (EPPR)

-0.578%	-1.388%	-0.664%	-3.391%
	-0.407%	-3.335%	-3.562%
		-4.088%	

Figure 14. Pin Power Error of EPPR w/o treatment at 30GWD/tU

RMS (FF)

1.573%	1.353%	1.564%	3.457%
	1.512%	1.948%	4.329%
		4.369%	

Max (FF)

4.011%	3.904%	4.313%	8.269%
	4.394%	4.718%	15.001%
		11.501%	

Min (FF)

-7.858%	-5.751%	-7.522%	-9.665%
	-7.425%	-7.175%	-10.422%
		-10.720%	

Figure 15. Pin Power Error of FF-PPR at 30GWD/tU

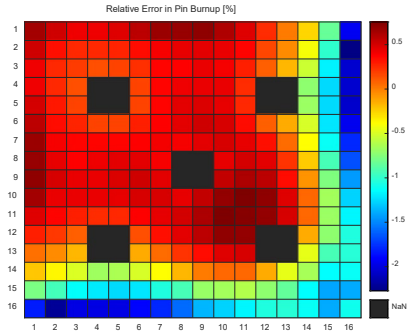

Figure 16. Pin Burnup Error of EPPR at 30GWD/tU

The relative error in pin-wise burnup for the fuel assembly with the largest RMS error is low enough to be acceptable. As burnup increases, the pin power error at the periphery increases slightly, but since the power density is significantly lower than the average, it does not cause serious issues.

In the EPPR method, the computation time was 91.59 seconds with Xe-135 and Sm-149 treatment and 76.47 seconds without it. The FF-PPR method took 10.13 seconds. It should be noted that the computing time includes nodal burnup calculations, and the EPPR algorithm has not been parallelized yet.

4. Conclusions

This study explores and compares two methods for burnup-dependent pin power reconstruction in a 2-D UOX PWR core, aiming to achieve a more accurate pin-wise power solution for a burned reactor core. The conventional FF-PPR and the EPPR methods were applied, with an additional assessment of the EPPR method's accuracy using a simplified estimation of pin-wise absorption cross sections, without iterative

measures. The results demonstrate that the EPPR method closely matches the reference solution, particularly in the peripheral regions across all burnup levels. Furthermore, it was confirmed that even without iterative calculations, the simplified estimation of absorption cross sections yields sufficiently accurate results. Future research will focus on developing methods to more accurately evaluate the burnup of fuel rods that contain burnable absorbers. Additionally, the potential integration of transient and thermal-hydraulic coupling with the EPPR method could be investigated.

REFERENCES

1. K. S. SMITH, "Assembly Homogenization Techniques for Light Water Reactor Analysis," *Prog. Nucl. Energy*, 17, 3, 303 (1986)
2. Han Gyu Joo et al., Multigroup pin power reconstruction with two-dimensional source expansion and corner flux discontinuity, *Annals of Nuclear Energy 36 (2009) 85–97*
3. Hwanyeal Yu, Seongdong Jang, and Yonghee Kim, "A New Embedded Analysis with Pinwise Discontinuity Factors for Pin Power Reconstruction", *Nuclear Science and Engineering,* 195:7, 766-777, 2021
4. Yunseok Jeong, Taesuk Oh, and Yonghee Kim, "Burnup-dependent Pin Power Reconstruction with Embedded Calculation", *M&C 2023*
5. J. Y. Cho, et al., "DeCART2D v1.0 Methodology Manual," KAERI/TR-5283/2013, Korea Atomic Energy Research Institute (2013).
6. Taesuk Oh, et al., "Development and validation of multiphysics PWR core simulator KANT", *Nuclear Engineering and Technology*, In-press, 2023.
7. J. KIM and Y. KIM, "Three-Dimensional Pin-Resolved Transient Diffusion Analysis of PWR Core by the Hybrid Coarse-Mesh Finite Difference Algorithm," *Nucl. Sci. Eng.*, 194, 1 (Jan. 2020);